

PCA-Assisted Local Flow Field Analysis and its Application in Aerodynamic Optimization

Kaiwen DENG *, Haixin CHEN ** and Yufei ZHANG ***

**School of Aerospace, Tsinghua University*

North Mengminwei Science Building, Tsinghua University, Haidian District, Beijing, China, 100084

Abstract

A hybrid optimization frame LFABO that embeds principle component analysis (PCA) technique into a common aerodynamic optimizer based on differential evolution and multi-layer perceptron meta-model is proposed in this paper. PCA approach is utilized as flow field analyser which dynamically extracts characteristics from flow field meta-data generated by CFD evaluations during the optimization process. Using those obtained characteristic descriptors of local flow fields, an integrated surrogate model concatenating design variables and concerned objectives can be established. Efficient optimization can then be conducted upon established surrogate models. The proposed approach is applied to an airfoil drag reduction process, preliminary results has revealed this approach's dominance over traditional surrogate-based optimization techniques in terms of solution quality and authenticity.

1. Introduction

Aerodynamic optimization, with distinctive patterns of expensive optimization, have experienced substantial development regarding optimization techniques during last decades. Approaches such as evolutionary algorithms (EA)[1–8], surrogate models[9–15], adjoint method combining gradient-based optimizers [16–24]and hybrid methods [25–28] are continuously proposed, examined and utilized in this field witnessing increasingly profound improvement in optimizers' performances.

However, aerodynamic optimization is still faced with the dilemma between local search efficiency and global search ability: common evolutionary algorithm-based optimization requires large amount of CFD evaluations towards convergence and gradient-based method can converge rapidly but suffers from trapping in local optimum. Robustness and uncertainty involved in the real-world application of aerodynamic optimization are also important issues which robust optimization[27,29–32] is aimed to solve, but the accompanying booming computation burden has aroused another concern. The key issue that causes aerodynamic optimization such straits is the expensive CFD evaluation process. Incorporation of surrogate model can well alleviate those computation burden by substituting time-consuming numerical analysis with a faster but less accurate alternative which can also filter the numerical error generated by numerical solver. Although there has been impressive development in surrogate models in recent years, enhancement strategies such as gradient-enhanced Kriging and co-Kriging are proposed and can well increase the prediction accuracy. However, while constructing the surrogate, information utilized is still constrained to peripheral level, i.e. only the design variables, concerned objectives and information directly related to them are used. The meta-data (flow field information and similar) generated by CFD solver depicting the fluid physics is usually discarded. Previous experience has shown that experienced and knowledgeable aerodynamic designers and experts can efficiently analyze those meta-data. By recognizing and predicting the fluid structures, experts are able to obtain feasible aerodynamic design within few rounds of experiments or numerical simulation.

With the development of data mining related technology, such process can be partly replaced by machine-learning aided in-depth analysis of the flow field. Massive information lies in the physics of aerodynamics and the obtained numerical data. There has been attempts to use data mining technologies in the field of aerodynamic optimization, but most of them are still analyzing data within variable-objective level, K.Chiba[33] utilized self-organizing map (SOM), rough set theory (RST) and ANOVA to analyse the correlation and trade-off relationship between objectives and variables from database generated in an EA-dominated aerodynamic optimization process. Zhendong Guo[34] used self-adaptive differential evolution to optimize a high pressure ratio centrifugal impeller and utilized SOM to carry out trade-off analysis between objectives and discovered design variables which have significant impact on concern objectives.

Moving deeper to analyse flow field meta-data can have great potential, possible benefits may lie in below areas where such analysis can be used to:

- (1). Accelerate CFD convergence or alleviate computation cost.
- (2). Accelerate optimization process by adding potential individuals with reasonable flow structure.
- (3). Enhance surrogate model to predict more accurately and physically.
- (4). Help establish the understanding of more complex fluid phenomena and promote theoretical development.

In this paper, an attempt has been made to adopt principal component analysis (PCA) or proper orthogonal decomposition (POD) technique as characteristic analyser of deliberately truncated flow field section of evaluated solutions to construct an enhanced surrogate model with higher accuracy and application potential. surrogate-based optimization (SBO) using differential evolution is then conducted, the whole process can be named as local flow-field analysis based optimization (LFABO). Comparisons are made to between LFABO and traditional SBO. Note that multi-layer perceptron (MLP) is selected as baseline surrogate model in this paper.

2. Local flow field analysis based optimization

2.1 Central idea introduction

The central idea of LFABO is to obtain and utilize the condensed low dimensional characteristics of the flow field generated during the optimization process, there are various ways capable to extract features from flow field, they are:

- (1). Unsupervised learning techniques such as PCA, SOM, or deep neural networks such as deep belief network (DBN) and auto encoder (AE).
- (2). Supervised learning techniques which includes feature extraction session such as convolution neural network.
- (3). Prior knowledge based feature extraction, which in the case of aerodynamic optimization refers to aerodynamics guided fluid structure recognition such as shock waves and flow separation.

Supervised learning is not suitable, for the features extracted are directly related to the selection of concerned objectives and thus can be rather subjective. Knowledge-based method is applicable, however the utilization of this approach is highly depending on the type of problems. In the case of 2 dimensional nozzle thrust optimization, it's clear that shock waves and expansion waves are significant, their intensity, location and appearance strongly affects the total thrust performance. But in other cases such as 3 dimensional aircraft drag reduction, concerned flow characteristics can be various kinds of vortex, flow separation, transition location and many other unknown or vague mechanisms. It's hard to form universal and intelligent solution to handle all possible occasions.

Here we propose PCA for two main reasons:

- (1). The dimension reduction process is explainable and understandable, for the low dimensional characteristics explicitly refers to the components of high dimensional base vectors while reconstructing the original flow field.
- (2). Its computation and storage cost is affordable.

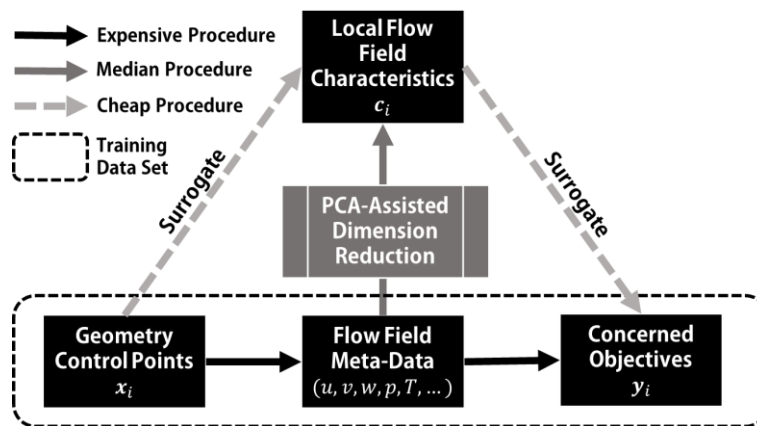


Figure 1: Surrogate construction in LFABO

2.2 LFABO framework

Assuming a database containing N_S samples with corresponding design variables x_i , objectives y_i ($i = 1, 2, \dots, N_S$) and related local flow field data has been previously obtained. PCA is firstly adopted to map the local flow field data into characteristics c_i . Then two multi-layer perceptron surrogate models S_1 and S_2 are constructed separately to map $\{x_i\}$

to $\{c_i\}$ and $\{c_i\}$ to $\{y_i\}$. An integrated surrogate S is then constructed by concatenating S_1 and S_2 . Differential evolution is then adopted as optimizer to search for the optimum solution upon S .

The introduction of differential evolution, PCA and MLP is introduced in section 3.

The procedures for construction of surrogate S is concluded in Figure 1:, and the total optimization framework compared to traditional SBO is shown in Figure 2:

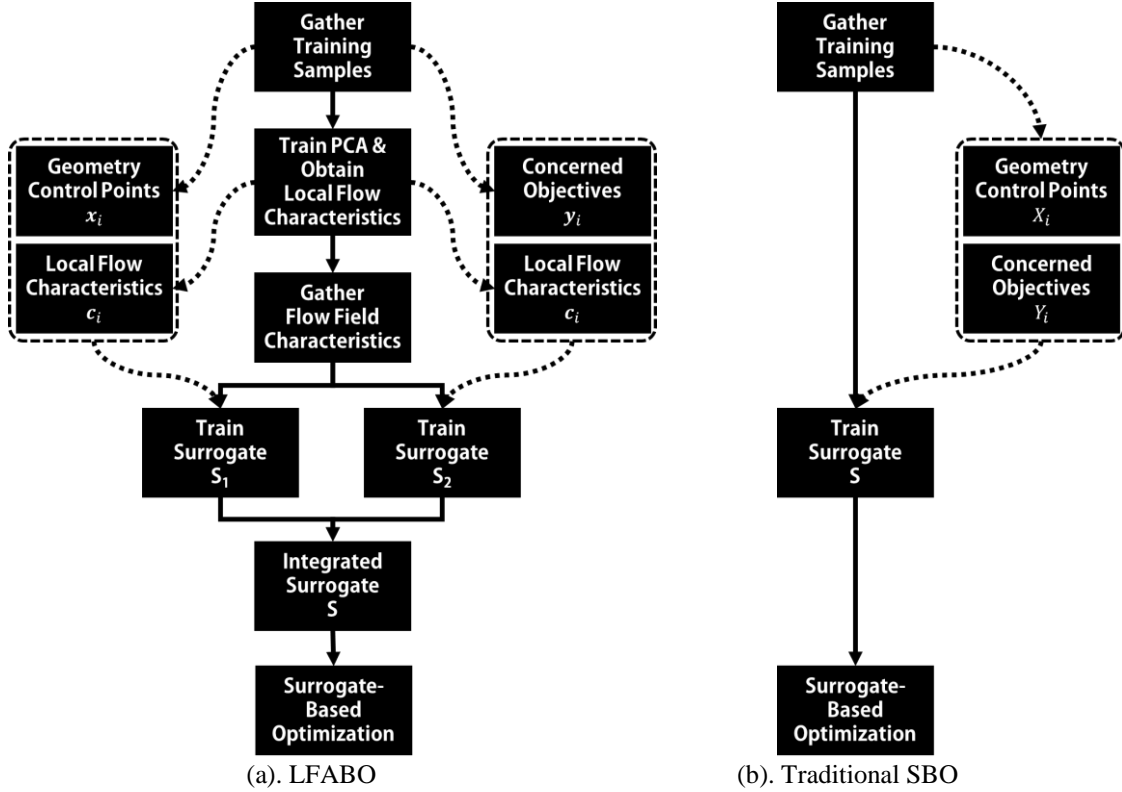


Figure 2: Optimization procedure comparison between LFABO and traditional SBO

3. Method introduction

3.1 Differential evolution

Differential evolution is a simple real-coded evolutionary algorithm used in continuous space optimization. Similar to Genetic Algorithm(GA), differential evolution has 3 main stages in each generation: mutation, crossover and selection. In case of confusion, here we combine design variables x and its corresponding objective functions $y = f(x)$ as an individual (x, y) . Population P^k is formed by individuals $P_i^k(x_i^k, y_i^k)$. For every individual-related expression, subscripts indicate the current generation while superscripts represent its index in the population. the basic processes of differential evolution can be concluded as such sequential operation to each individual from parent population $P_i^k(x_i^k, y_i^k)$:

(1). Select n base vectors $x_{r1}^k, x_{r2}^k, \dots, x_{rn}^k$ out from the current population's individuals' design variables and execute mutation operator, obtain the corresponding mutated individual of P_i^k as $V_i^k(v_i^k, f(v_i^k))$. and be noted that $f(v_i^k)$ is left uncalculated. The mutation process can have several variants described as formulations in equation (1) ~ (4) in which the number after slash k symbols the pair of individuals needed to mutate, and we have $n = 2k$.

$$\text{Rand}/1 : v_i^k = x_i^k + F \times (x_{r2}^k - x_{r3}^k) \quad (1)$$

$$\text{Rand}/2 : v_i^k = x_i^k + F \times (x_{r2}^k - x_{r3}^k + x_{r4}^k - x_{r5}^k) \quad (2)$$

$$\text{Best}/1 : v_i^k = x_{best}^k + F \times (x_{r1}^k - x_{r2}^k) \quad (3)$$

$$\text{Best}/2 : v_i^k = x_{best}^k + F \times (x_{r1}^k - x_{r2}^k + x_{r3}^k - x_{r4}^k) \quad (4)$$

(2). Execute crossover operation using the mutated individual $V_i^k(v_i^k, f(v_i^k))$ and its corresponding parent individual

$P_i^k(x_i^k, y_i^k)$ to generate the corresponding trial individual $U_i^k(u_i^k, f(u_i^k))$.

(3). Calculate $f(u_i^k)$, execute selection operation between $U_i^k(u_i^k, f(u_i^k))$ and $P_i^k(x_i^k, y_i^k)$ to filter the better one to be settled in the offspring population as $P_i^{k+1}(x_i^{k+1}, y_i^{k+1})$.

All these three main procedures have multiple variants during different utilizations which enables DE to be variable and adjustable. We could uniquely mark a certain DE as DE/a/b/c while “a” and “b” symbol the mutation scheme, as have described above. “c” represents the crossover scheme and can be classified into binary crossover and exponential crossover[35]. Above procedures are concluded in Figure 3:

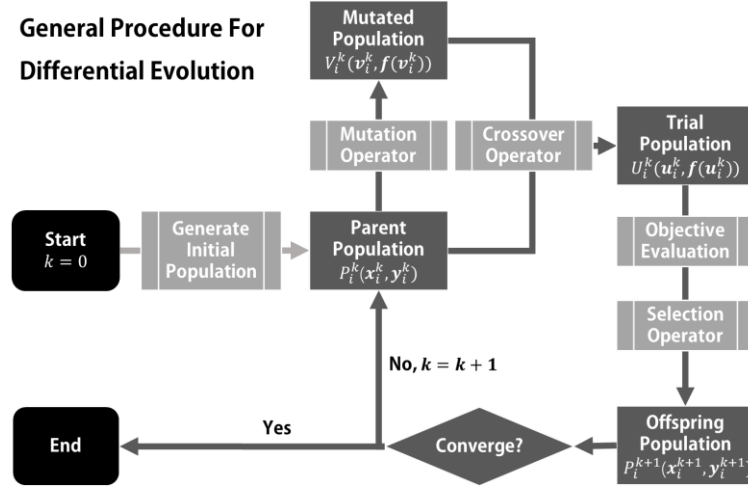


Figure 3: Optimization procedures of differential evolution

3.2 Multi-layer perceptron

Multi-layer perceptron (MLP) is perhaps the best known and well used artificial neural network surrogate model in aerodynamic optimization. MLP refers to feedforward neural network which contains one or more hidden layer. MLP structure that owns only one hidden layer can be depicted in Figure 4. N_x and N_y refer to the dimension of design variables and objectives, or in other words the input and output dimension. N_H refers to the number of nodes in hidden layer, which is usually a function of N_x . Nodes in adjacent layers of MLP are connected one by one with weight w_{ij} , which refers to the connection strength of i^{th} node in the preceding layer and j^{th} node in the back layer.

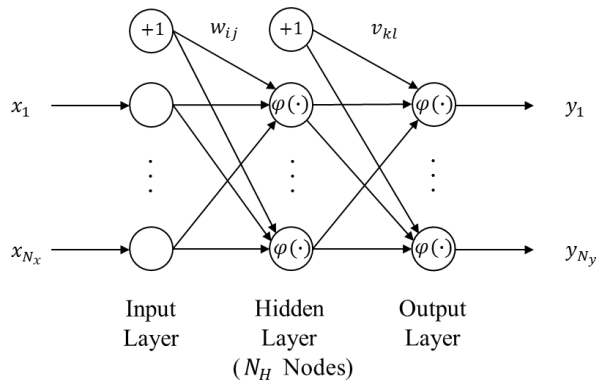


Figure 4: MLP structure containing one hidden layer

MLP contains three types of layers: input layer, hidden layer and output layer. Both hidden layer and output layer obtain the weighted sum of the input given by their preceding layer and pass the result into a non-linear activation function φ as the output to the next layer. Taking the structure shown in Figure 1 for example, assuming node i from the hidden layer produces output p_i , the mapping relationship between layers can be depicted as:

$$\text{Hidden Layer: } p_i = \varphi_i \left(\sum_{j=1}^{N_H} w_{ji} x_j + w_{j0} \right) \quad (5)$$

$$\text{Output Layer: } y_i = \varphi_i \left(\sum_{j=1}^{N_Y} v_{ji} p_j + v_{j0} \right) \quad (6)$$

Most commonly used φ_i are tanh, ReLU and Sigmoid function, they can be defined as equation (7)~(10) where k , k_1 and k_2 are positive parameters :

$$\text{TanH: } \varphi(x) = \frac{e^x - e^{-x}}{e^x + e^{-x}} \quad (7)$$

$$\text{ReLU: } \varphi(x) = \begin{cases} 0 & x < 0 \\ kx & x \geq 0 \end{cases} \quad (8)$$

$$\text{Leaky ReLU: } \varphi(x) = \begin{cases} k_1x & x < 0 \\ k_2x & x \geq 0 \end{cases} \quad (9)$$

$$\text{Sigmoid: } \varphi(x) = \frac{1}{1 + e^{-x}} \quad (10)$$

Regarding construction of MLP, the training process is significant. The main purpose and very essence of training is to endow MLP the ability to simulate unknown black-box functions on both known training set and unknown test set. Back propagation algorithm is the most frequently used and efficient method to train MLP. It gives a form where the partial derivatives of total training error to each parameters that need to be tuned can be conveniently and efficiently calculated. Back propagation is usually incorporated with gradient based optimization approach such as Newton-Raphson method, stochastic gradient descent and others.

3.3 Principal component analysis

PCA is a statistical approach to transform observations correlated variables into a set of components of linearly uncorrelated base vectors. This method is adopted to carry out local flow field analysis and dimension reduction. Assuming a series of high dimensional training data $\{\mathbf{o}_i\}$, $i = 1, \dots, N_S$ ($\dim(\mathbf{o}_i) = N_o$) have been collected, PCA manages to find the intrinsic connection between different dimensions of each training data as well as between different samples and represents those samples in a pithy way.

Suggesting that $N_S > N_o$, we can create the data matrix \mathbf{D} by putting \mathbf{o}_i in column's order as:

$$\mathbf{D} = [\mathbf{o}_1 - \boldsymbol{\mu}, \mathbf{o}_2 - \boldsymbol{\mu}, \dots, \mathbf{o}_{N_S} - \boldsymbol{\mu}] \quad (11)$$

$$\text{Where } \mathbf{o}_i = [o_{i1}, o_{i2}, \dots, o_{iN_o}]^T, \boldsymbol{\mu} = (\sum_{i=1}^{N_S} \mathbf{o}_i) / N_S$$

PCA aims to find m ($m < N_o$) base vectors which best represent the spacial distribution of training data, or the observation of unknown variables, in the design hyperspace. Those vectors are then used to map the original high dimensional data into lower dimensions or the inverse. The selection of such base vectors requires such characteristics: Firstly, high dimensional data that's recovered from low dimensional characteristics should preserve as greater variance as possible and covariance between different dimension of low dimensional characteristics should be zero. Regarding those requirements, we can obtain the base vectors following procedure (1) ~ (3):

(1). Calculate the covariance matrix of the original data set.

$$\mathbf{C} = \frac{1}{N_o} \mathbf{D} \cdot \mathbf{D}^T \quad (12)$$

(2). Compute the eigen-matrix \mathbf{P}_0 and eigen-values λ_i (stored in diagonal matrix $\boldsymbol{\lambda}$) of the covariance matrix depicted in equation (13), note that λ_i are sorted in an descending order by its absolute value.

$$\mathbf{C} \mathbf{P}_0^T = \mathbf{P}_0 \boldsymbol{\lambda} \quad (13)$$

$$\text{Where } \mathbf{P}_0 = [\mathbf{p}_1, \mathbf{p}_2, \dots, \mathbf{p}_n]^T, \mathbf{p}_i = [p_{i1}, p_{i2}, \dots, p_{in}]^T$$

$$\text{And } \boldsymbol{\lambda} = \begin{bmatrix} \lambda_1 & \dots & 0 \\ \vdots & \ddots & \vdots \\ 0 & \dots & \lambda_{N_x} \end{bmatrix}$$

(3). Eigen-value λ_i indicates the amount of variance information preserved through inverse transformation from the low dimensional data on the i^{th} base, so the eigen-vector \mathbf{p}_i ($i = 1, 2, \dots, m$) which relates to the greatest m eigen-values are selected as the base vectors, and for any given observation \mathbf{o}^* , its low dimensional characteristic \mathbf{c}^* and recovered representation \mathbf{r}^* can be obtained via equation (14) ~ (15) as shown below:

$$\mathbf{c}^* = \mathbf{P}(\mathbf{o}^* - \boldsymbol{\mu}) \quad (14)$$

$$\mathbf{r}^* = \mathbf{P}^T \mathbf{c}^* + \boldsymbol{\mu} \quad (15)$$

Where $\mathbf{P} = [\mathbf{p}_1, \mathbf{p}_2, \dots, \mathbf{p}_m]^T$

4. Flow solver validation

An in-house developed flow solver NSAWET based on window-embedment technology is used for flow analysis[36,37]. Here we illustrate the comparison between experiment data[38] and NSAWET calculated results on airfoil RAE2822 with 12.1% thickness. The detailed description of the experiment and CFD calculation setting is summarized in Table 1 and Table 2.

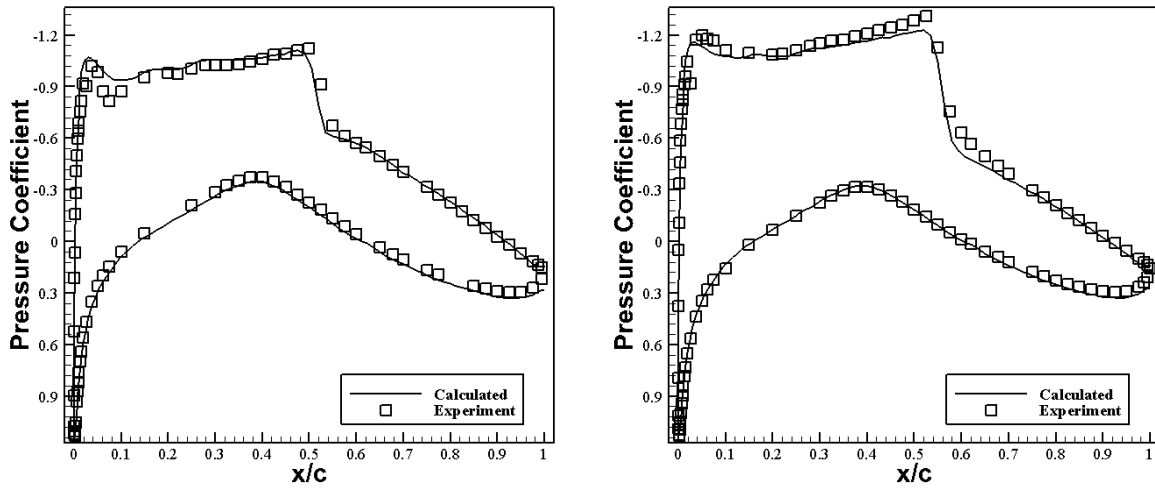
Figure 5: shows the comparison of calculated and experimental pressure distribution. It can be carefully concluded that NSAWET prediction is rather accurate.

Table 1: Experiment condition

Case No.	Case Index	Angle of Attack α	Reynolds Number Re	Mach Number Ma
1	7	2.55	6,500,000	0.725
2	9	3.19	6,500,000	0.730

Table 2: CFD setting

Grid Size	Reconstruction Scheme	Discretization Scheme	Turbulent Model
97×257	3rd order MUSCL	Roe	$k - \omega$ SST



a). Case 7

b). Case 9

Figure 5: Calculated and experimented pressure distribution on RAE2822 with 12.1% thickness

5. Test case validation

In this section the practical example of the proposed method is presented. A previously obtained airfoil database is used for training and testing. An airfoil single-point drag reduction optimization processes based on LFABO and pure MLP models are illustrated and compared.

5.1 Case settings

The airfoil is generated using total amount of 14 control points on the upper and lower surface with thickness set to be constant 12%. The working condition, calculation setting and optimization problem description are summarized in 0

Table 3: Working condition

Mach number Ma	Fixed lift coefficient C_L	Reynolds number Re
0.74	0.65	6,500,000

Table 4: CFD setting

Discretization scheme	Reconstruction scheme	Turbulence model
Roe	3 rd order MUSCL	$k - \omega$ SST

Table 5: Optimization description

Design variable x	Objective y	Constraints
14 Control points' position	Drag coefficient C_d at $Ma = 0.74$	None

The database contains 854 airfoil shapes along with corresponding surface pressure distribution, geometry control point coordinates and drag coefficient under the same working condition, among which 600 samples are used for training and the rest are used for testing. Three optimization configurations (named A, B and C) are compared, among which A and B both adopt LFABO with minor differences in surrogate structure, and C is traditional MLP based optimization, the MLP structure is shown in Figure 6:

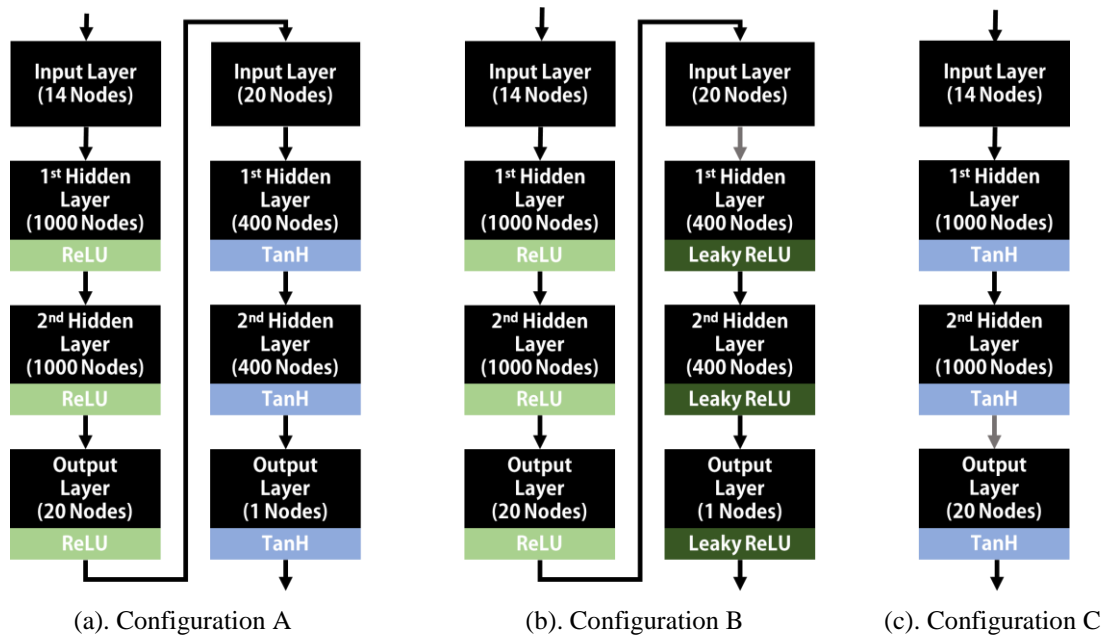


Figure 6: Surrogate model structure

5.2 Test procedure and result

As shown in Figure 2: Firstly the database is obtained by executing geometry and grid generation followed by numerical analysis using NSAWET. For proposed LFABO method, the PCA is trained to map the high dimensional flow field data into low dimensional flow field characteristics c_i . Two MLP surrogates S_1 and S_2 are trained simultaneously to construct the integrated surrogate S .

Figure 7: shows the original flow field of 6 randomly picked samples and the corresponding recovered flow field.

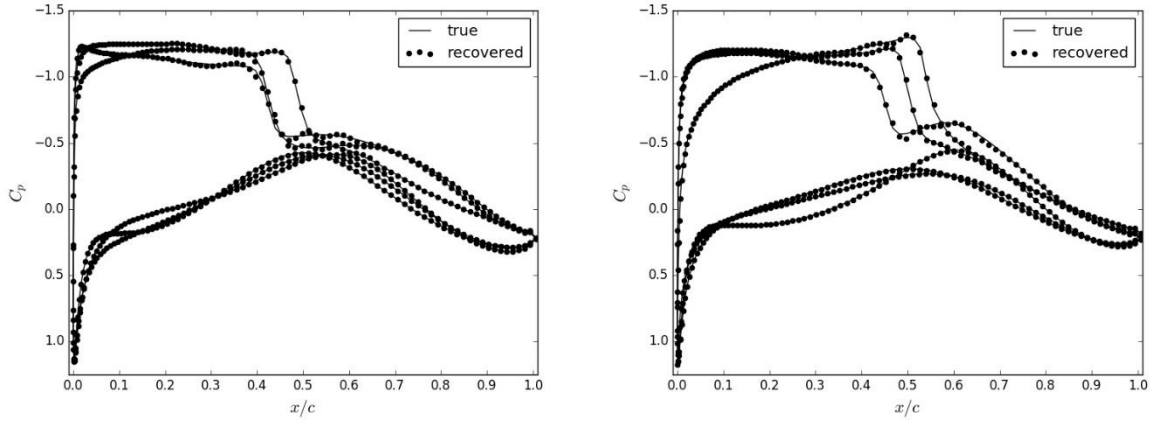


Figure 7: PCA recovery performance

Regarding the training session, back propagation associated with stochastic gradient descent is adopted, total training steps are 250,000. The learning rate is initialized as 10^{-2} and descends to $1/10$ after every 50,000 steps. Final prediction error of the integrated surrogate on test samples in configuration A is around 4.97% while the configuration B is around 5.18% with moderate difference. The prediction error is defined as:

$$e = \sum_{i=1}^{N_T} (Y_i - P_i)^2 / N_T \quad (16)$$

Where N_T symbols the test set size, P_i symbols the prediction given by the surrogate while input is X_i . Differential evolution is adopted as the main optimizer, the optimizer setting is concluded in Table 6:

Table 6: Differential evolution optimizer setting

Population size	Total generation	Mutation scheme	Crossover scheme	Mutation rate	Crossover rate	Total objective evaluation
100	100	Rand/1	Binary	0.50	0.20	Around 10,000

Figure 8: shows the converging history of the surrogate-based optimization on configuration A, B and C, the vertical axis shows the mean Euclidean distance from the current population to the final optimal solution. After nearly 10,000 surrogate predictions, all three configurations can give stable optimal prediction. Figure 9: shows the optimum shape and validated pressure distribution of the optimum shapes obtained.

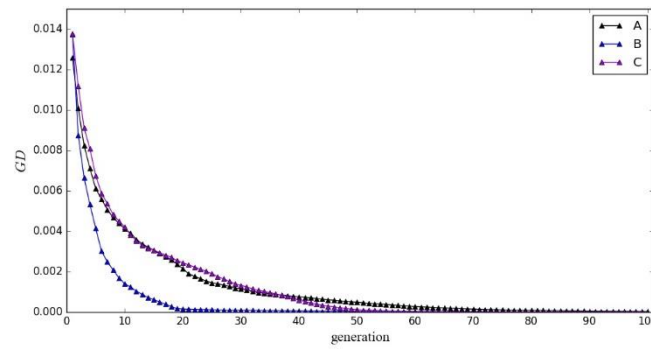


Figure 8: Optimization convergence history

Table 7: Objective validation

	Configuration A	Configuration B	Configuration C
Predicted C_d	7.93397E-3	1.05185E-2	7.87919E-3
Validated C_d	1.13715E-2	1.14684E-2	1.26535E-2

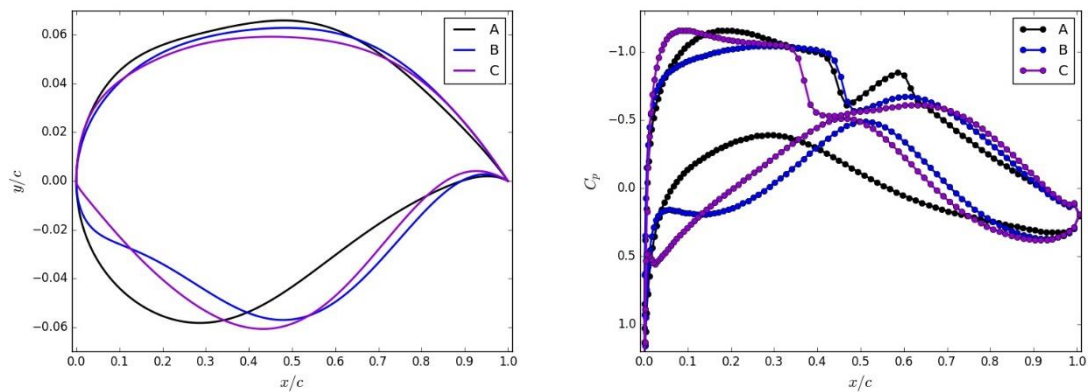


Figure 9: Optimum shape and pressure distribution

5.3 Result discussion

From Figure 9:, it can be observed that the optimal shape obtained by configuration B has an obvious bump near the leading edge on the lower surface, which directly leads to the second acceleration on the same area. Optimal shape obtained by configuration C has very small leading edge radius, and the curvature transition is nearly discontinuous, which leads to the second acceleration near the leading edge and low pressure peak on the lower surface. Optimal shape obtained by configuration A has second acceleration on the upper surface, however its shock wave intensity appears to be the smallest.

From Table 7: it can be concluded that configuration A and B owns the best optimization result, the validated drag coefficient is far less than that of configuration C. This result validates the effectiveness of the proposed flow field analysis based optimization method in enhancing surrogate model's accuracy.

6. Conclusion

A flow field analysis based optimization frame LFABO that further exploits meta data generated during the optimization process using PCA, DE and MLP is proposed and presented. Compared to traditional surrogate-based optimization, LFABO has such features:

- (1). The test error can be partly reduced.
 - (2). The prediction is more accurate, optimization based on it is more reliable.
- However, more validation needs to be done test the proposed method's performance in more aerodynamic optimization cases. The intrinsic cause of the observed accuracy improvement of surrogates should also be carefully investigated.

References

- [1] Mosetti G, P. C. 1993. Aerodynamic Shape Optimization by Means of a Genetic Algorithm. In: *5th Int. Symp. Comput. Fluid Dyn.* 297–284.
- [2] Obayashi, S., and Takanashi, S. 1995. Genetic Algorithm for Aerodynamic Inverse Optimization Problems. In: *First International Conference on IET.* 7–12.
- [3] Obayashi, S., and Tsukahara, T. 1997. Comparison of Optimization Algorithms for Aerodynamic Shape Design. *AIAA J.* 35(8):1413–1415.
- [4] Vicini, A., and Quagliarella, D. 1997. Inverse and Direct Airfoil Design Using a Multiobjective Genetic Algorithm, *AIAA J.* 35(9):1499–1505.
- [5] Vicini, A., and Quagliarella, D. 1997. Multipoint Transonic Airfoil Design by Means of a Multiobjective Genetic Algorithm. In: *35th Aerosp. Sci. Meet.*
- [6] Jones, B. R., Crossley, W. a., and Lyrintzis, A. S. 2000. Aerodynamic and Aeroacoustic Optimization of Rotorcraft Airfoils via a Parallel Genetic Algorithm. *J. Aircr.* 37(6):1088–1096.
- [7] Oyama, A., Obayashi, S., and Nakahashi, K. 2001. Real-Coded Adaptive Range Genetic Algorithm Applied to Transonic Wing Optimization. *Appl. Soft Comput.* 1:179–187.
- [8] Zingg, D. W., Nemec, M., and Pulliam, T. H. 2008. A Comparative Evaluation of Genetic and Gradient-Based Algorithms Applied to Aerodynamic Optimization. In: *Eur. J. Comput. Mech. Eur. Mécanique Numérique.* 17(1–2):103–126.
- [9] Giunta, A. 1997. Aircraft Multidisciplinary Design Optimization Using Design of Experiments Theory and Response Surface Modeling Methods. PhD Thesis. Virginia Polytechnic Inst. and State Univ.
- [10] Simpson, T. W., Mauery, T. M., Korte, J. J., and Mistree, F. 2001. Kriging Models for Global Approximation in Simulation-Based Multidisciplinary Design Optimization. *AIAA J.* 39(12):2233–2241.
- [11] Jeong, S., Murayama, M., and Yamamoto, K. 2005. Efficient Optimization Design Method Using Kriging Model. *J. Aircr.*, 42(2):413–420.
- [12] Forrester, A., and Keane, A.. 2009. Recent Advances in Surrogate-Based Optimization. *Prog. Aerosp. Sci.* 1–77.
- [13] Saijal, K. K., Ganguli, R., and Viswamurthy, S. R. 2011. Optimization of Helicopter Rotor Using Polynomial and Neural Network Metamodels. *J. Aircr.* 48(2):553–566.
- [14] Han, Z., and Görtz, S. 2012. Hierarchical Kriging Model for Variable-Fidelity Surrogate Modeling. *AIAA J.* 50(9): 1885–1896.
- [15] Andrés-Pérez, E., Carro-Calvo, L., Salcedo-Sanz, S., and Martin-Burgos, M. J. 2016. *Application of Surrogate-Based Global Optimization to Aerodynamic Design.* Springer.
- [16] Jameson, A. 1995. Optimum Aerodynamic Design Using CFD and Control Theory. *AIAA Pap.* 1729:124–131.
- [17] Burgreen, G. W., and Baysal, O. 1996. Three-Dimensional Aerodynamic Shape Optimization Using Discrete Sensitivity Analysis. *AIAA J.* 34(9):1761–1770.
- [18] Reuther, J., Jameson, A., Farmer, J., Martinelli, L., and Saunders, D. 1996. Aerodynamic Shape Optimization of Complex Aircraft Configurations via an Adjoint Formulation. *AIAA Pap.* 94.
- [19] Elliott, J., and Peraire, J. 1997. Practical Three-Dimensional Aerodynamic Design and Optimization Using Unstructured Meshes. *AIAA J.* 35(9):1479–1485.
- [20] Elliott, J., and Peraire, J. 1997. Aerodynamic Optimization on Unstructured Meshes with Viscous Effects. *AIAA Pap.* 97:1849.
- [21] Kim, S., Alonso, J. J., and Jameson, A. 1999. A Gradient Accuracy Study for the Adjoint-Based Navier-Stokes Design Method. *AIAA Pap.* 299.
- [22] Reuther, J. J., Jameson, A., Alonso, J. J., Rimlinger, M. J., and Saunders, D. 1999. Constrained Multipoint Aerodynamic Shape Optimization Using an Adjoint Formulation and Parallel Computers, Part 2. *J. Aircr.* 36(1):61–74.
- [23] Nadarajah, S., and Jameson, A. 2000. A Comparison of the Continuous and Discrete Adjoint Approach to Automatic Aerodynamic Optimization. *AIAA Pap.* 667:2000.
- [24] Kim, S. K., Alonso, J. J., and Jameson, A. 2000. Two-Dimensional High-Lift Aerodynamic Optimization Using the Continuous Adjoint Method. *AIAA Pap.* 4741(8).
- [25] Poloni, C., Giurgevich, A., Onesti, L., and Pediroda, V. 2000. Hybridization of a Multi-Objective Genetic Algorithm, a Neural Network and a Classical Optimizer for a Complex Design Problem in Fluid Dynamics. *Comput. Methods Appl. Mech. Eng.* 186(2–4):403–420.

- [26] Kim, H. 2010. Aerodynamic Optimization Using a Hybrid MOGA-Local Search Method. In: *51st AIAA/ASME/ASCE/AHS/ASC Structures, Structural Dynamics, and Materials Conference*.
- [27] Epstein, B., and Peigin, S. 2004. Robust Hybrid Approach to Multiobjective Constrained Optimization in Aerodynamics. *AIAA J.* 42(8):1572–1581.
- [28] Hacioglu, A. 2007. Fast Evolutionary Algorithm for Airfoil Design via Neural Network. *AIAA J.* 45(9):2196–2203.
- [29] Padulo, M., Campobasso, M. S., and Guenov, M. D. 2011. Novel Uncertainty Propagation Method for Robust Aerodynamic Design. *AIAA J.* 49(3):530–543.
- [30] Jiangtao, H., Zhenghong, G., Ke, Z., and Junqiang, B. 2010. Robust Design of Supercritical Wing Aerodynamic Optimization Considering Fuselage Interfering. *Chinese J. Aeronaut.* 23(5):523–528.
- [31] Shimoyama, K., Oyama, A., and Fujii, K. 2006. Robust Aerodynamic Airfoil Design Optimization Against Wind Variations for Mars Exploratory Airplane. In: *57th Int. Astronaut. Congr.* 2–4.
- [32] Dodson, M., and Parks, G. T. 2009. Robust Aerodynamic Design Optimization Using Polynomial Chaos. *J. Aircr.* 46:635–646.
- [33] Chiba, K., and Obayashi, S. 2008. Knowledge Discovery for Flyback-Booster Aerodynamic Wing Design Using Data Mining. *J. Spacecr. Rockets.* 45(5):975–987.
- [34] Guo, Z., Song, L., Zhou, Z., Li, J., and Feng, Z. 2015. Multi-Objective Aerodynamic Optimization Design and Data Mining of a High Pressure Ratio Centrifugal Impeller. *J. Eng. Gas Turbines Power.* 137(9):92602.
- [35] Storn, R., and Price, K. 1997. Differential Evolution – A Simple and Efficient Heuristic for Global Optimization over Continuous Spaces. *J. Glob. Optim.* 11(4):341–359.
- [36] Chen, H. X., Fu, S., and Li, F. W. 2003. Navier-Stokes Simulations for Transport Aircraft Wing/body High-Lift Configurations. *J. Aircr.* 40(5):883–890.
- [37] Zhang, Y., Chen, H., and Fu, S. 2011. Improvement to Patched Grid Technique with High-Order Conservative Remapping Method. *J. Aircr.* 48(3):884–893.
- [38] Cook, P. H., McDonald, M. A., and Firmin., M. C. .1979. *Aerofoil RAE 2822 - Pressure Distributions, and Boundary Layer and Wake Measurements*.